Readiness in Formation Control of Multi-Robot System

Zhihao Xu, Hiroaki Kawashima and Klaus Schilling

***Abstract*— To analyze the performance of the formation system in response to inputs/disturbances from outside of the formation, we propose the notion of *readiness*, which describes the initial conditions of the formation in terms of a certain set of input space. A higher readiness means better initial conditions of the system with better performance in maintaining or recovering the original formation shape against the exogenous inputs/disturbances. Optimization method based on calculus of variations is used in the analysis for deriving the optimality conditions. Simulations modeled on both unicycle and car-like robots demonstrate the features and the potential applications of the proposed notion.**

I. Introduction

There have been a great number of studies on multi-agent team coordination and distributed sensor networks, where a decentralized control law was proposed to solve different cooperative tasks, such as consensus, line deployment, space coverage, shape forming, and target converging [1], [2], [3], [4]

In particular, distance-based robot formation control successfully achieves deployment of multi-agents (e.g. robots) and tracking of target in formation without using the knowledge of global coordinates [5], [6], [7]. Once desired distances of selected agent pairs are given, the agents can form a designed formation in a decentralized manner, where the control laws for individual agents are obtained based on the negative gradient of a global index (sometimes referred to as formation constraint function, potential function, or edge-tension energy). A model-independent coordination strategy was proposed in [5], and is applied to the path following problem by using a nonphysical virtual leader that tracks a desired trajectory. Stability properties for distance-based formation stabilization of both single and double integrator agents are studied in [6], which is further extended to nonholonomic mobile robots in [7].

Apart from the control law and stability of the system, the agents' initial conditions, as one important aspect in multi-agent systems, also determine the overall performance of the mission to accomplish. Especially, in distance-based formation control, the relation between the response of the system and some conditions such as agents' positions and network topologies has attracted attention of researchers [8], [9], [10]. In [8], the notion of *stiffness* and the related *rigidity indices* are proposed to evaluate the rate of convergence to the original formation after the agents' positions are perturbed. In [9], the *approximate manipulability* of leader-follower networks is proposed to characterize the effective agent positions, topologies, and directions of leader's movements in terms of instantaneous response of the system to the leader's input. These notions are further unified in [10] as the *responsiveness*.

This work is supported by the Elitenetwork of Bavaria through the program "Identification, Optimization and Control with Applications in Modern Technologies".

Z. Xu and K. Schilling are with the Department of Computer Science VII: Robotics and Telematics, University of Würzburg, Germany. E-Mail: {xu,schi}@informatik.uni-wuerzburg.de. K. Schilling is also leader of the Zentrum für Telematik, Würzburg, Germany. Hiroaki Kawashima is with the Graduate School of Informatics, Kyoto University, Japan. E-Mail: kawashima@i.kyoto-u.ac.jp

However, the previously proposed notions strongly depend on the assumption of single-integrator models. Meanwhile, for real robotic applications, other states of agents, such as heading directions of nonholonomic agents (e.g. unicycle and car-like models), have to be taken into account. For example, when a multi-agent system tracks a moving point, one can ask a question such as "given topology and positions of a car-like multi-agent system, what are the optimal initial headings for the agents to effectively respond to a point with unpredictable movement?" Here, the existing indices, such as rigidity and responsiveness, cannot be used due to the nonholonomity of the agents. As such, a different notion of the performance measure is required.

In this paper, we address the optimal initial conditions of a multi-robot formation system by introducing the notion of *Readiness*, which interprets how well the system is prepared for a variety of external disturbances (also considered as exogenous inputs in the context of this paper). We illustrate this notion by optimizing the set of initial orientations of the robots, so that they can respond to the external disturbances coming from any direction in the plane and recover the formation with minimum difference in the shape change.

The rest of the paper is structured as follows: Section II introduces the problem of interest, formulates the approach and proposes a new notion that can be used to better understand how to solve the problem. Section III and Section IV presents two case studies of the unicycle and car-like robot models that illustrate the meaning of this notion, with the simulation results shown in Section V. Finally, Section VI concludes the paper with a few remarks and future works.

II. Problem Statement and Readiness Formulation

Given a group of N agents, with $x_i(t) \in \mathbb{R}^d$ being the state of agent i at time t, $i = 1, \dots, N$. Let the agent with the last index be assigned as the leader and the remaining $N_f = N - 1$ agents as followers, i.e., $x_l \triangleq x_N$ is the leader's state, and $x_f = [x_1^\top, \dots, x_{N_f}^\top]^\top$ are the follower states. The overall system configuration of the network can be denoted by $x \triangleq [x_1^\top, ..., x_N^\top]^\top = [x_f^\top, x_l^\top]^\top$.

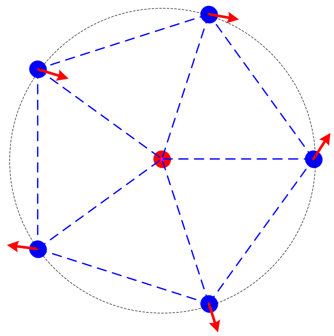

Fig. 1. Convoy Protection Scenario; blue discs are the unicycle robots, with their headings indicated by the red arrows; the red disc in the middle is the object to protect; blue dashed lines represent communication links.

Suppose the dynamics of the agents are given by:

$$\dot{x}(t) = f(x(t), u), \tag{1}$$

with the initial states $x(0) = x_0$, where $u \in U$ is the exogenous input to the formation system, usually applied onto the leader. For instance, the system dynamics can be separated as:

$$\dot{x}(t) = \begin{bmatrix} \dot{x}_f(t) \\ \dot{x}_l(t) \end{bmatrix} = \begin{bmatrix} f_f(x) \\ f_l(x_l, u) \end{bmatrix}, \tag{2}$$

where the input u has no direct influence on the followers. Now the problem is to find the optimal initial condition x_0^* of the system in terms of how well the system responds to arbitrary input $u \in U$, where u acts as a constant exogenous input in a given short-term interval $[0, T]$. In other words, we would like to see how the total system is prepared for a variety of perturbation, parameterized by u, given through the leader.

To illustrate this problem, we consider an exemplary scenario where a group of mobile robots perform convoy protection of an object, as shown in Fig. 1. The robots are evenly located on a circle, with the object of interest at its centroid. In order to protect this object, the convoy is expected to move as quickly as possible to recover the shape of even distribution on a circle with the object still at its centroid, in case that the object moves in some direction on the plane. In order to characterize this ability of the formation, we introduce the notion called *readiness*, which is defined in the following.

First, we consider the standard cost functional used for optimal initial condition problem in the form:

$$\tilde{J}(x_0, u) = \int_0^T L(x(t), u)dt + \Psi(x(T), u), \tag{3}$$

where $L(x(t), u)$ is a cost function on states and input u. $\Psi(x(T), u)$ is a terminal cost function. For instance, it can be used to punish the difference between desired formation shape and the shape at time T.

Now we define the *readiness* by taking the integral (parameterized family) of cost functionals $\{\tilde{J}(x_0, u) | u \in U\}$ to evaluate the overall response of the system. Specifically, the following cost functional is defined for readiness:

$$J(x_0) = \int_U \left(\int_0^T L(x(t), u)dt + \Psi(x(T), u) \right) du. \tag{4}$$

$J(x_0)$ punishes the general integral and terminal costs under inputs $u \in U$. If $J(x_0)$ is small, then the system with the corresponding x_0 has high readiness. In the convoy protection scenario, this means the formation is better prepared for external disturbances and recovers faster to the original shape.

To optimize the readiness, the optimal initial condition x_0^* is given by:

$$\begin{aligned} x_0^* &= \arg\min_{x_0} J(x_0) \\ \text{s.t.} \quad \dot{x}(t) &= f(x(t), u) \\ x(0) &= x_0. \end{aligned}$$

We take the advantage of the integration form of u in Eq. (4), and therefore, using calculus of variations, we get the first-order necessary condition (FONC) as (see Appendix I)

$$\frac{\partial J}{\partial x_0} = \int_U \lambda^\top(0, u)du = 0 \tag{5}$$

where

$$\begin{cases} \dot{\lambda}(t, u) & = -\dfrac{\partial L}{\partial x}^\top (x(t), u) - \dfrac{\partial f}{\partial x}^\top (x(t), u)\lambda(t, u) \\ \lambda(T, u) & = \dfrac{\partial \Psi}{\partial x(T)}^\top (x(T), u) \end{cases} \tag{6}$$

with the costate $\lambda \in \mathbb{R}^{dN}$.

In the rest of the paper, we analyze the optimal readiness of nonholonomic multi-robot formation for such a convoy protection scenario shown in Fig. 1. This problem is interpreted as to solve the readiness for initial headings of the mobile robots in the convoy, supposing their initial positions satisfy the formation shape.

III. System Modeling

Before we can find the optimal initial headings, we need to introduce our control strategy, which is often referred to as edge-tension energy based formation control.

A. Edge-Tension Energy [10]

Consider the graph $\mathsf{G} = (\mathsf{V}, \mathsf{E})$ for Fig. 1, where $\mathsf{V} = \{\mathsf{v}_1, \ldots, \mathsf{v}_N\}$ denotes the set of robots and object in the graph, and $\mathsf{E} \subseteq \mathsf{V} \times \mathsf{V}$ is the set of edges, indicated by the blue dashed lines. The cardinality of E is $|\mathsf{E}| = M$, which is the number of edges in the graph. Now we introduce a general edge-tension energy similar to the formulation in [10]:

$$E(x) = \frac{1}{2} \sum_{i=1}^N \sum_{j=1}^N E_{ij}(x_i(t), x_j(t)), \tag{7}$$

where

$$E_{ij}(x_i, x_j) = \begin{cases} \frac{1}{2} \left(e_{ij}(||x_i - x_j||)\right)^2 & \{\mathsf{v}_i, \mathsf{v}_j\} \in \mathsf{E} \\ 0 & \text{otherwise.} \end{cases} \tag{8}$$

Here, $e_{ij} : \mathbb{R}_+ \to \mathbb{R}$ is a strictly increasing, twice differentiable function such that $e_{ij}(d_{ij}) = 0$ and $e'_{ij}(d_{ij}) \neq 0$, where $d_{ij} > 0$ is the desired distance between agents i and j, and $e'_{ij}(r) \triangleq \frac{de_{ij}(r)}{dr}$. A typical example of e_{ij} is

$$e_{ij}(||x_i - x_j||) = c_{ij} \cdot (||x_i - x_j|| - d_{ij}), \qquad (9)$$

where $c_{ij} > 0$ is a weight variable assigned to the communication link between agents i and j.

Let $D(\mathsf{G}) \in \{-1, 0, 1\}^{N\times M}$ be an incidence matrix [11] of graph G. The first and the second derivatives of the edge-tension energy is given by the followings (see [9] for the details of the derivation):

$$\begin{aligned}
\frac{\partial E(x)}{\partial x}^\top &= ((DW_1(x)D^\top) \otimes I_d)x, \\
\frac{\partial^2 E(x)}{\partial x^2} &= (DW_1(x)D^\top) \otimes I_d + R(x)^\top W_2(x)R(x)
\end{aligned}$$

where $W_1(x)$ and $W_2(x)$ are $M \times M$ diagonal matrices, whose diagonal elements are

$$\begin{aligned}
[W_1(x)]_{kk} &= w_{i_k j_k}(||x_{i_k} - x_{j_k}||), \\
[W_2(x)]_{kk} &= \frac{w'_{i_k j_k}(||x_{i_k} - x_{j_k}||)}{||x_{i_k} - x_{j_k}||}, \\
& \quad k = 1, ..., M, \quad \{\mathsf{v}_{i_k}, \mathsf{v}_{j_k}\} : \text{edge } k,
\end{aligned}$$

where, letting $e''_{ij}(r) \triangleq \frac{d^2 e_{ij}(r)}{dr^2}$,

$$\begin{aligned}
w_{ij}(r) &\triangleq \frac{e_{ij}(r)e'_{ij}(r)}{r}, \\
w'_{ij}(r) &\triangleq \frac{dw_{ij}}{dr} = \frac{\{e'_{ij}(r)^2 + e_{ij}(r)e''_{ij}(r)\}r - e_{ij}(r)e'_{ij}(r)}{r^2}.
\end{aligned}$$

Here we assume that the indices of the edges are consistent between $W_1(x)$ and the incidence matrix D, and between $W_2(x)$ and the rigidity matrix R, respectively.

Remark 1: If all the desired distances are satisfied at $x = x^*$, then $\frac{\partial E}{\partial x}\big|_{x^*} = 0$ and

$$\left.\frac{\partial^2 E}{\partial x^2}\right|_{x^*} = R(x^*)^\top W_2(x^*)R(x^*). \qquad (10)$$

By the definition of the function e_{ij} and the fact that $||x_i - x_j|| = d_{ij} > 0$ at $x = x^*$, $W_2(x^*)$ is always positive definite.

Example 1: If the edge-tension energy is given by (9), then $e'_{ij}(r) = c_{ij}$, $e''_{ij}(r) = 0$, $[W_1(x)]_{kk} = c^2_{i_k j_k}(1 - d_{i_k j_k}/||x_{i_k} - x_{j_k}||)$, and $[W_2(x)]_{kk} = c^2_{i_k j_k} d_{i_k j_k}/||x_{i_k} - x_{j_k}||^3$. Hence, when the desired distances are satisfied at $x = x^*$, the k-th diagonal elements of the weight matrices become

$$[W_1(x^*)]_{kk} = 0, \quad [W_2(x^*)]_{kk} = \left(\frac{c_{i_k j_k}}{d_{i_k j_k}}\right)^2. \qquad (11)$$

B. Formation Control with Unicycle Models

Edge-tension energy based formation control was applied to agents with single integrator dynamics in [9]. The formation control was realized according to the following dynamics:

$$\mu_i(x) \triangleq \dot{x}_i = -\frac{\partial E}{\partial x_i}^\top(x) = -\sum_{j\in N_i} w_{ij}(x_i - x_j). \qquad (12)$$

In terms of the followers, the dynamics can be derived as:

$$\dot{x}_f = -\frac{\partial E}{\partial x_f}^\top(x) = -((D_f W_1(x)D^\top) \otimes I_2)x, \qquad (13)$$

where $D_f \triangleq [I_{N_f}|0]D$ (the last row of D is removed).

Now consider the unicycle model given by:

$$\begin{aligned}
\dot{x}_i &= \begin{bmatrix}\cos\theta_i \\ \sin\theta_i\end{bmatrix} v_i \\
\dot{\theta}_i &= \omega_i
\end{aligned}, \qquad (14)$$

where θ_i is the heading of agent i, v_i and ω_i are the linear and angular velocities, respectively. Due to the nonholonomic constraints of the unicycle model, we will control the off-center point $\tilde{x}_i$ (in order to have complete controllability of the model) defined as:

$$\tilde{x}_i = x_i + \epsilon \begin{bmatrix}\cos\theta_i \\ \sin\theta_i\end{bmatrix}, \qquad (15)$$

where $\epsilon > 0$. Taking time derivative, we have

$$\dot{\tilde{x}}_i = \dot{x}_i + \epsilon \begin{bmatrix}-\sin\theta_i \\ \cos\theta_i\end{bmatrix}\dot{\theta}_i = \begin{bmatrix}\cos\theta_i & -\sin\theta_i \\ \sin\theta_i & \cos\theta_i\end{bmatrix}\begin{bmatrix}v_i \\ \epsilon\omega_i\end{bmatrix} \qquad (16)$$

Therefore the control input $[v_i, \omega_i]$ to achieve $\dot{\tilde{x}}_i = \mu_i$ is given by

$$\begin{bmatrix}v_i \\ \omega_i\end{bmatrix} = \begin{bmatrix}\cos\theta_i & \sin\theta_i \\ -\frac{1}{\epsilon}\sin\theta_i & \frac{1}{\epsilon}\cos\theta_i\end{bmatrix}\mu_i = \begin{bmatrix}p_1(\theta_i)^\top \\ \frac{1}{\epsilon}p_2(\theta_i)^\top\end{bmatrix}\mu_i, \qquad (17)$$

where

$$p_1(\theta_i) \triangleq [\cos\theta_i, \sin\theta_i]^\top, p_2(\theta_i) \triangleq [-\sin\theta_i, \cos\theta_i]^\top.$$

Substituting (17) into the original unicycle model (14), we have the following closed-loop system

$$\begin{aligned}
\dot{x}_i &= p_1(\theta_i)v_i = p_1(\theta_i)p_1(\theta_i)^\top\mu_i(x) \\
\dot{\theta}_i &= \frac{1}{\epsilon}p_2(\theta_i)^\top\mu_i(x)
\end{aligned}. \qquad (18)$$

With the definition given in Eq. (12) for the control input $\mu_i(x)$, the follower system can be described as follows:

$$\begin{cases}
\dot{x}_f = f_x(x, \theta_f) \triangleq -P_1(\theta_f)P_1(\theta_f)^\top \frac{\partial E}{\partial x_f}^\top(x) \\
\dot{\theta}_f = f_\theta(x, \theta_f) \triangleq -\frac{1}{\epsilon}P_2(\theta_f)^\top \frac{\partial E}{\partial x_f}^\top(x)
\end{cases} \qquad (19)$$

where $\theta_f = [\theta_1, ..., \theta_{N_f}]^\top$, and the matrices $P_1, P_2 \in \mathbb{R}^{2N_f\times N_f}$ are defined as

$$P_j(\theta_f) \triangleq \begin{bmatrix}p_j(\theta_1) & & & \\ & p_j(\theta_2) & & \\ & & \ddots & \\ & & & p_j(\theta_{N_f})\end{bmatrix}, \qquad (20)$$

where $j = 1, 2$. Here, we suppose that the movement of the leader (i.e. object) is given externally. In particular, the control law given in Eq. (19) locally asymptotically stabilizes the formation to the desired shape. This is formulated in the following proposition.

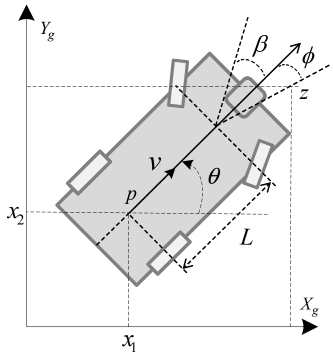

Fig. 2. Model of car-like mobile robot

Proposition 1 (Unicycle formation stabilization): The formation system with unicycle model given in Eq. (14) is locally stable under the control law given in Eq. (19).

Proof: Consider the candidate Lyapunov function:

$$V(x) = E(x),$$

where $E(x)$ is the edge-tension energy defined in Eq. (7). Differentiating V in time and we get:

$$\begin{aligned}\dot{V} = \dot{E} = \frac{\partial E}{\partial x_f}\dot{x}_f &= -\frac{\partial E}{\partial x_f} P_1(\theta_f) P_1(\theta_f)^\top \frac{\partial E}{\partial x_f}^\top \\ &= -\left\| P_1(\theta_f)^\top \frac{\partial E}{\partial x_f}^\top \right\|^2 \leq 0.\end{aligned} \tag{21}$$

Therefore, the control law given in Eq. (19) ensures stability of the system. ■

While in general the control law in Eq. (19) may drive the system toward a local equilibrium point, we here consider only small perturbations of the agents from their desired formation such that the desired distances are recovered, where the desired formation can be defined by the set X^*:

$$X^* \triangleq \{x \in \mathbb{R}^{2N} | \|x_i - x_j\| = d_{ij}, \{\mathsf{v}_i, \mathsf{v}_j\} \in \mathsf{E}\}. \tag{22}$$

Based on Remark 1 and Example 1, we know $\|x_i - x_j\| = d_{ij} \Rightarrow \dot{V} = 0$. Therefore, the set X^* is one equilibrium set.

This proposition shows that the distances between the agents will be driven to the desired ones (if initial states are in the neighborhood of the set X^*), although the control law (19) has no guarantee for the convergence of the headings of the agents. In the following, we are going to design a similar control law for the car-like robot models.

C. Formation Control on Car-like Mobile Robots

Consider the vehicle in the formation as a standard rear-wheel drive, front-wheel steerable car-like mobile robot, whose kinematic equation is given by:

$$\begin{bmatrix}\dot{x}_{1i}(t)\\ \dot{x}_{2i}(t)\\ \dot{\theta}_i(t)\end{bmatrix} = \begin{bmatrix}\cos\theta_i(t)\\ \sin\theta_i(t)\\ [\tan\beta_i(t)]/L\end{bmatrix} v_i(t), \tag{23}$$

where v_i is the translational driving speed; β_i is the equivalent steering angle of the front wheels; (x_{1i}, x_{2i}) is the coordinate of the robot in global frame, located at the mid-point of the rear-wheel axle; θ_i is the orientation; and L is the distance between front and rear wheel axle. Note that the first two equations represent the nonholonomic constraints of the car-like mobile robot. And because of the nonholonomity, we control the off-center point z_i, defined by [12]:

$$z_i = \begin{bmatrix}x_{1i} + L\cos(\theta_i) + \epsilon\cos(\theta_i - \phi)\\ x_{2i} + L\sin(\theta_i) + \epsilon\sin(\theta_i - \phi)\end{bmatrix}, \tag{24}$$

where $-\frac{\pi}{2} < \phi < \frac{\pi}{2}$ is the off-center angle, and $\epsilon > 0$. Similar to the analysis on unicycle model, we can write the car-like robot dynamics in Eq. (23) for the follower system in stacked form:

$$\begin{cases}\dot{x}_f &= g_x(x, \theta_f)\\ &\triangleq -\dfrac{1}{1+\epsilon\cos(\phi)} P_1(\theta_f) P_3(\theta_f)^\top \dfrac{\partial E}{\partial x_f}^\top(x)\\ \dot{\theta}_f &= g_\theta(x, \theta_f)\\ &\triangleq -\dfrac{1}{1+\epsilon\cos(\phi)} P_2(\theta_f)^\top \dfrac{\partial E}{\partial x_f}^\top(x)\end{cases} \tag{25}$$

where $P_3 \in \mathbb{R}^{2N_f \times N_f}$ is defined as:

$$P_3(\theta_f) \triangleq \begin{bmatrix}p_3(\theta_1) & & & \\ & p_3(\theta_2) & & \\ & & \ddots & \\ & & & p_3(\theta_{N_f})\end{bmatrix}, \tag{26}$$

and

$$p_3(\theta_i) \triangleq [\cos(\theta_i) + \epsilon\cos(\theta_i - \phi), \sin(\theta_i) + \epsilon\sin(\theta_i - \phi)]^\top. \tag{27}$$

We also suppose that the movement of the leader (object) in the centroid is given externally. In particular, this control law given in Eq. (25) locally asymptotically stabilizes the car-like robot formation to the desired shape, which can be proved similarly to that of Proposition 1, where the same Lyapunov candidate is used. We omit the derivation for brevity.

IV. Readiness Optimization

Following the scenario shown in Fig. 1, and the system dynamics with unicycle model given in Eq. (14) and control law given by Eq. (19), suppose the system initial configuration satisfies the desired distances with

$$x = x^* = \begin{bmatrix}x_f^*\\ x_l^*\end{bmatrix},$$

where $\|x_i - x_j\| = d_{ij}, \forall\{\mathsf{v}_i, \mathsf{v}_j\} \in \mathsf{E}$. Note that the edge set E represents the communication link shown in Fig. 1, which does not change in time. Let δx_l be the instantaneous movement of the leader, given by:

$$\delta x_l = \gamma \begin{bmatrix}\cos\theta_l\\ \sin\theta_l\end{bmatrix}, \tag{28}$$

where $\gamma > 0$, and θ_l is the direction of the movement. Suppose that the leader will not move after this displacement, i.e.,

$$x(0) = x^* + \begin{bmatrix}0\\ \delta x_\ell\end{bmatrix}, \quad x(t) = x^* + \begin{bmatrix}\delta x_f(t)\\ \delta x_\ell\end{bmatrix}, \tag{29}$$

where $\delta x_f(t) \triangleq x_f(t) - x_f^*$.

We are going to analyze the readiness of the system, namely the set of initial headings of all followers, associated with the cost given below:

$$J(x_0) = \int_U \Psi(x(T), u) du, \tag{30}$$

where we let $L = 0$ in Eq. (4), since we only focus on the final formation shape for simplicity. An example of $f(x,u)$ and $\Psi(x,u)$ is $\dot{x} = -\frac{\partial E}{\partial x}^\top(x,u)$ and $E(x(T),u)$, respectively. The exogenous input u is defined as the direction of the movement of the object in the centroid, i.e.

$$u \triangleq \theta_l, \text{ and } U \triangleq [0, 2\pi].$$

In this case, $J(x_0)$ is an index to measure the change of edge-tension energy E in the system under all the given $u \in U$.

The optimal initial condition problem in terms of optimizing the readiness of the system depicted in Fig. 1 is given by:

$$\begin{aligned} \min_{\theta_0} \quad & J(\theta_0) = \int_0^{2\pi} \Psi(x(T), u) du \qquad (31)\\ \text{s.t.} \quad & \dot{x} = \begin{bmatrix} \dot{x}_f \\ \dot{x}_l \end{bmatrix} = \begin{bmatrix} f_x(x, \theta_f, u) \\ 0 \end{bmatrix} \\ & x_f(0) = x_f^*, \quad \theta_f(0) = \theta_0 \\ & x_l(0) = \delta x_l, \quad \theta_l(0) = \theta_l \end{aligned}$$

where $\Psi(x(T), u) = E(x(T), u)$. Using calculus of variations, we get the FONC as

$$\frac{\partial J}{\partial \theta_0} = \int_0^{2\pi} \lambda^\top(0, u) du = 0, \tag{32}$$

where

$$\begin{cases} \dot{\lambda}(t, u) & = -\dfrac{\partial f}{\partial x}^\top(x(t), u)\lambda(t, u) \qquad (33a) \\ \lambda(T, u) & = \dfrac{\partial \Psi}{\partial x(T)}^\top(x(T), u) \qquad (33b) \end{cases}$$

Specifically, the derivation of FONC for both unicycle and car-like models can be found in Appendix II.

V. Results

Solving the optimal control problem given in Eq. (31) numerically in MATLAB® based on the following gradient descent principle:

$$\theta_0^{(k+1)} = \theta_0^{(k)} - \eta \frac{\partial J}{\partial \theta_0}^\top, \tag{34}$$

where η is the step size and k is the iteration count. Although the method of gradient descent does not give global solution, we noticed that through multiple simulations, the "Tangential" setup of the headings is more probable to be the optimal solution. Therefore, our initial guess is set to be "Tangential", where all follower headings are tangential to the circle of convoy. If the initial guess is far from tangential, the result might be some other local minimum. Note that the results shown in this section apply to both unicycle and car-like models, since the control law itself is based on the same formulation of edge-tension energy introduced in Section III-A.

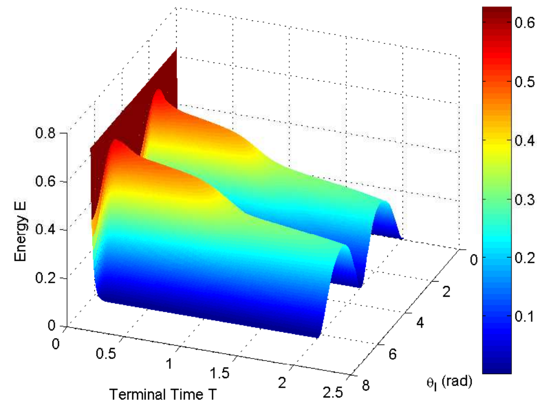

Fig. 3. Edge-tension energy distribution with uniform heading; θ_l is used in Eq. (28) to generate instantaneous movement of the leader, which is also considered as the exogenous input.

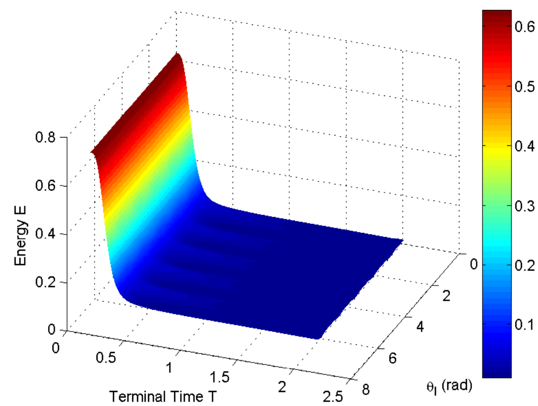

Fig. 4. Edge-tension energy distribution with optimal initial heading

Fig. 3 shows distribution of the edge-tension energy E when the initial headings of the followers are uniformly aligned as $\theta_0 = \mathbf{0}$. The local minima shown in the figure indicate that the formation system is "ready" for the leader's movement in the direction of $\theta_l = 0$ and $\theta_l = \pi$, but is not "ready" when the leader moves in any other direction. Therefore, the overall "readiness" is low in terms of the cost J given in Eq. (31) (which is also shown in Fig. 5).

Fig. 4 illustrate the edge-tension energy distribution when initial headings of the followers are placed with the solution to the optimal control problem given in Eq. (31). Clearly, the energy E is decreased along all directions of the leader's movement. This means that the system with the optimal set of headings has high readiness.

Fig. 5 depicts the cost J given in Eq. (31) under different sets of initial headings, which also indicates the readiness of the system. The curve marked "Optimal" shows the cost J with optimal initial headings, which is slightly smaller than the one with "Tangential" after approximately 0.2 time units. An interesting observation is that the uniform and random headings result in a very low cost in the beginning of the formation recovering. This comes from the fact that

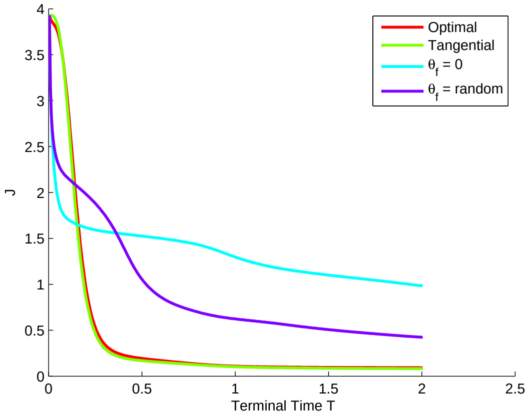

Fig. 5. Cost comparison

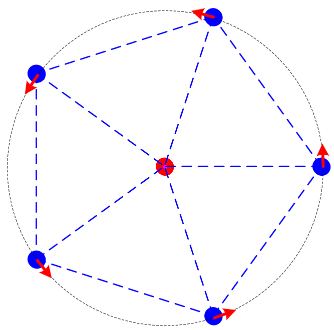

Fig. 6. Optimal Initial Headings of the Convoy; the red arrows indicate the headings.

the uniform heading setup has very low cost along $\theta_l = 0$ and $\theta_l = 2\pi$ direction, as shown in Fig. 3. The integration of the cost over $[0, 2\pi]$ benefits from this, and thus the cost drops really fast in the beginning. However, the costs for "Optimal" and "Tangential" headings approach zero much faster, which indicates higher readiness for these two initial conditions.

The optimal headings calculated numerically are depicted in Fig. 6. The difference of this "Optimal" setup from the "Tangential" one is ca. 2.1 deg to the inner side of the circle. This also reflects the fact that the tangential initial heading is nearly optimal. In the case where the formation needs to be moving or circling around the center object, the tangential heading can behave just as well.

VI. Conclusion

In this paper, we have introduced the notion of *readiness* to describe the initial conditions of a formation system in terms of how well the system is prepared for a given set of input space that consists of a variety of external disturbances. We analyzed the optimal readiness and its first-order necessary condition over a given input space, and applied the result to a formation of nonholonomic mobile robots. It successfully characterizes the optimal initial headings of the unicycle and car-like robots for the case where the robots try to keep the circular formation shape when the external disturbances come from any direction in the plane. More examples to demonstrate the usefulness of this notion will be studied in the future.

Acknowledgments

The authors would like to thank Dr. Magnus Egerstedt, School of Electrical and Computer Engineering, Georgia Institute of Technology, for his enlightening suggestions to this paper.

References

[1] J.T. Feddema, R.D. Robinett, and R.H. Byrne. An optimization approach to distributed controls of multiple robot vehicles. In *Workshop on Control and Cooperation of Intelligent Miniature Robots, IEEE/RSJ International Conference on Intelligent Robots and Systems*, 2003.

[2] R. Olfati-Saber and R.M. Murray. Distributed structural stabilization and tracking for formations of dynamic multi-agents. In *Proceedings of the 41st IEEE Conference on Decision and Control, 2002*, pages 209–215, Las Vegas, Nevada, USA, Dec. 2002.

[3] A. Jadbabaie, J. Lin, and A.S. Morse. Coordination of groups of mobile autonomous agents using nearest neighbor rules. *IEEE Transactions on Automatic Control*, 48(6):988–1001, 2003.

[4] F. Bullo, J. Cortés, and S. Martinez. *Distributed control of robotic networks: a mathematical approach to motion coordination algorithms*. Princeton Univ Pr, 2009.

[5] M. Egerstedt and X. Hu. Formation constrained multi-agent control. *IEEE Transactions on Robotics and Automation*, 17(6):947–951, 2001.

[6] D.V. Dimarogonas and K.H. Johansson. On the stability of distance-based formation control. In *Proceedings of the 47th Conference on Decision and Control*, pages 1200–1205, Cancun, Mexico, Dec. 2008.

[7] D.V. Dimarogonas and K.H. Johansson. Further results on the stability of distance-based multi-robot formations. In *Proceedings of American Control Conference. ACC'09.*, pages 2972–2977, St. Louis, MO, USA, Jun. 2009.

[8] Y. Kim, G. Zhu, and J. Hu. Optimizing formation rigidity under connectivity constraints. In *Proceedings of the 49th IEEE Conference on Decision and Control (CDC)*, pages 6590–6595, Atlanta, GA, USA, Dec. 2010.

[9] H. Kawashima and M. Egerstedt. Approximate manipulability of leader-follower networks. In *Proceedings of 50th IEEE Conference on Decision and Control and European Control Conference*, pages 6618–6623, Florida, USA, Dec. 2011.

[10] H. Kawashima, G. Zhu, J. Hu, and M. Egerstedt. Responsiveness and manipulability of formations of multi-robot networks. In *Proceedings of 51st IEEE Conference on Decision and Control*, pages 4622– 4628, Maui, Hawaii, USA, Dec. 2012.

[11] M. Mesbahi and M. Egerstedt. *Graph Theoretic Methods in Multiagent Networks*. Princeton University Press, 2010.

[12] A. De Luca, G. Oriolo, and C. Samson. Feedback control of a nonholonomic car-like robot. *Robot motion planning and control*, page 200, 1998.

Appendix I
First-order Necessary Condition (FONC) for Optimal Readiness

Since the input u is a constant over a short time interval, and we are taking integration of this input over the entire input space U for the system dynamics given in Eq. (1), in order to avoid ambiguity, we denote the system state as $x(t, u)$ in the following derivation to point out that x depends on u implicitly.

Taking the constraint in Eq. (1) into account, we consider the cost functional

$$\hat{J}(x_0) = \int_U \Bigg[\int_0^T \Big\{ \lambda(t,u) \Big(f(x(t,u),u) - \dot{x} \Big) + L(x(t,u),u) \Big\} dt + \Psi(x(T,u),u) \Bigg] du. \quad (35)$$

Suppose that a small change, $x_0 + \epsilon h$, in the initial condition causes a small change, $x(t,u) + \epsilon\eta(t,u)$, in the state trajectory, where $\epsilon > 0$. Then,

$$\begin{aligned}
&\hat{J}(x_0 + \epsilon h) \\
&= \int_U \Bigg[\int_0^T \Big\{ L(x(t,u) + \epsilon\eta(t,u), u) \\
&+ \lambda(t,u)\Big(f(x(t,u) + \epsilon\eta(t,u), u) - (\dot{x} + \epsilon\dot{\eta}) \Big) \Big\} dt \\
&+ \Psi(x(T,u) + \epsilon\eta(T,u), u) \Bigg] du. \qquad (36)
\end{aligned}$$

Due to the linearity of integration, the following difference can be calculated with the Taylor expansions of L, f, and Ψ:

$$\begin{aligned}
&\hat{J}(x_0 + \epsilon h) - \hat{J}(x_0) \\
&= \int_U \Bigg[\int_0^T \Big\{ \frac{\partial L}{\partial x}\epsilon\eta(t,u) + \lambda(t,u)\frac{\partial f}{\partial x}\epsilon\eta(t,u) \\
&\quad - \epsilon\lambda(t,u)\dot{\eta} \Big\} dt + \frac{\partial \Psi}{\partial x}\epsilon\eta(T,u) \Bigg] du + o(\epsilon) \\
&= \epsilon \int_U \Bigg[\int_0^T \Big\{ \frac{\partial L}{\partial x}\eta(t,u) + \lambda(t,u)\frac{\partial f}{\partial x}\eta(t,u) \\
&\quad + \dot{\lambda}\eta(t,u) \Big\} dt - \lambda(T,u)\eta(T,u) + \lambda(0,u)\eta(0,u) \\
&\quad + \frac{\partial \Psi}{\partial x(T,u)}\eta(T,u) \Bigg] du + o(\epsilon), \qquad (37)
\end{aligned}$$

where the last equality follows from integration by parts,

$$\int_0^T \lambda(t,u)\dot{\eta} dt = [\lambda(t,u)\eta(t,u)]_0^T - \int_0^T \dot{\lambda}\eta(t,u) dt. \quad (38)$$

Dividing (37) by ϵ and taking the limit $\epsilon \to 0$, we obtain the directional derivative

$$\begin{aligned}
\delta\hat{J}(x_0; h) &= \lim_{\epsilon \to 0} \frac{\hat{J}(x_0 + \epsilon h) - \hat{J}(x_0)}{\epsilon} \\
&= \int_U \left[\int_0^T \left\{ \frac{\partial L}{\partial x} + \lambda\frac{\partial f}{\partial x} + \dot{\lambda} \right\} \eta(t,u) dt \right. \\
&\quad \left. + \left\{ \frac{\partial \Psi}{\partial x(T,u)} - \lambda(T,u) \right\} \eta(T,u) \right] du \\
&\quad + \int_U \lambda(0,u)\eta(0,u) du. \qquad (39)
\end{aligned}$$

Combining the costate dynamics from Eq. (6), we have

$$\delta\hat{J}(x_0; h) = \int_U \lambda(0,u)\eta(0,u) du = \left(\int_U \lambda(0,u) dt \right) h, \quad (40)$$

where we used the fact $\eta(0,u) = h$, i.e., the change of initial value $x_0 + \epsilon h$ corresponds to $x(0,u) + \epsilon\eta(0,u)$. Noting the fact $\delta\hat{J}(x_0; h) = \frac{\partial \hat{J}}{\partial x_0} h$, the first-order necessary condition is given by Eq. (5).

Appendix II
FONC for Unicycle and Car-like Models

A. Unicycle Models

Based on the dynamics of unicycle models given in Eq. (19), dynamics of the costate $\lambda = [\lambda_x^\top, \lambda_\theta^\top]^\top \in \mathbb{R}^{2N_f \times N_f}$ can be described as:

$$\lambda_x(T, \theta_l) = \frac{\partial E}{\partial x_f}^\top (x(T), \theta_l), \qquad \lambda_\theta(T, \theta_l) = 0 \quad (41)$$

$$\begin{aligned}
\dot{\lambda}_x &= -\frac{\partial f_x}{\partial x_f}^\top \lambda_x - \frac{\partial f_\theta}{\partial x_f}^\top \lambda_\theta \\
&= \frac{\partial^2 E}{\partial x_f^2} \left(P_1 P_1^\top \lambda_x + \frac{1}{\epsilon} P_2 \lambda_\theta \right) \qquad (42)
\end{aligned}$$

$$\begin{aligned}
\dot{\lambda}_\theta &= -\frac{\partial f_x}{\partial \theta_f}^\top \lambda_x - \frac{\partial f_\theta}{\partial \theta_f}^\top \lambda_\theta \\
&= \left[\frac{\partial E}{\partial x_f} \right] \left((P_1 P_2^\top + P_2 P_1^\top)\lambda_x - \frac{1}{\epsilon} P_1 \lambda_\theta \right) \qquad (43)
\end{aligned}$$

where

$$\left[\frac{\partial E}{\partial x_f} \right] \triangleq \begin{bmatrix} \frac{\partial E}{\partial x_1} & & & \\ & \frac{\partial E}{\partial x_2} & & \\ & & \ddots & \\ & & & \frac{\partial E}{\partial x_{N_f}} \end{bmatrix}. \quad (44)$$

Specifically, the first order necessary condition becomes:

$$\frac{\partial J}{\partial \theta_0}^\top = \int_0^{2\pi} \lambda_\theta(0, \theta_l) d\theta_l = 0. \quad (45)$$

B. Car-like Models

Based on the dynamics of car-like robot models derived in Eq. (25), dynamics of the costate $\xi = [\xi_x^\top, \xi_\theta^\top]^\top \in \mathbb{R}^{2N_f \times N_f}$ can be described as:

$$\xi_x(T, \theta_l) = \frac{\partial E}{\partial x_f}^\top (x(T), \theta_l), \qquad \xi_\theta(T, \theta_l) = 0 \quad (46)$$

$$\begin{aligned}
\dot{\xi}_x &= -\frac{\partial f_x}{\partial x_f}^\top \xi_x - \frac{\partial f_\theta}{\partial x_f}^\top \xi_\theta \\
&= \eta \frac{\partial^2 E}{\partial x_f^2} \left(P_3 P_1^\top \xi_x + P_2 \xi_\theta \right) \qquad (47)
\end{aligned}$$

$$\begin{aligned}
\dot{\xi}_\theta &= -\frac{\partial f_x}{\partial \theta_f}^\top \xi_x - \frac{\partial f_\theta}{\partial \theta_f}^\top \xi_\theta \\
&= \eta \left[\frac{\partial E}{\partial x_f} \right] \left((P_3 P_2^\top + P_4 P_1^\top)\xi_x - P_1 \xi_\theta \right) \qquad (48)
\end{aligned}$$

where

$$\eta = \frac{1}{1 + \epsilon\cos(\phi)}, \qquad P_4 = P_2(\theta_f) + \epsilon P_2(\theta_f - \phi).$$

Specifically, the first order necessary condition becomes:

$$\frac{\partial J}{\partial \theta_0}^\top = \int_0^{2\pi} \xi_\theta(0, \theta_l) d\theta_l = 0. \quad (49)$$